

Elastic and piezoelectric moduli of Nd and Sm ferroborates

Cite as: Low Temp. Phys. **41**, 614 (2015); <https://doi.org/10.1063/1.4929719>

Published Online: 31 August 2015

T. N. Gaydamak, I. A. Gudim, G. A. Zvyagina, I. V. Bilych, N. G. Burma, K. R. Zhekov, and V. D. Fil



View Online



Export Citation



CrossMark

ARTICLES YOU MAY BE INTERESTED IN

[Direct and inverse magnetoelectric effects in \$\text{HoAl}_3\(\text{BO}_3\)_4\$ single crystal](#)

Journal of Applied Physics **115**, 174103 (2014); <https://doi.org/10.1063/1.4874270>

LOW TEMPERATURE TECHNIQUES
OPTICAL CAVITY PHYSICS
MITIGATING THERMAL
& VIBRATIONAL NOISE

[DOWNLOAD THE WHITE PAPER](#)

downloads.montanainstruments.com/optical_cavities

MONTANA INSTRUMENTS
COLD SCIENCE MADE SIMPLE



Elastic and piezoelectric moduli of Nd and Sm ferroborates

T. N. Gaydamak

B. I. Verkin Institute of Low-temperature Physics and Engineering, National Academy of Sciences of Ukraine, pr. Lenina 47, Kharkov 61103, Ukraine

I. A. Gudim

L. V. Kirenskii Institute of Physics, Siberian Branch of the Russian Academy of Sciences, Akademgorodok 50, Krasnoyarsk 660036, Russia

G. A. Zvyagina, I. V. Bilych, N. G. Burma, K. R. Zhekov, and V. D. Fil^(a)

B. I. Verkin Institute of Low-temperature Physics and Engineering, National Academy of Sciences of Ukraine, pr. Lenina 47, Kharkov 61103, Ukraine

(Submitted April 21, 2015)

Fiz. Nizk. Temp. **41**, 792–797 (August 2015)

The sound speeds are measured and the elastic and piezoelectric moduli are calculated for single crystal $\text{NdFe}_3(\text{BO}_3)_4$ and $\text{SmFe}_3(\text{BO}_3)_4$. These compounds are characterized by enhanced rigidity in the base plane with respect to stress-strain deformations and by a rather strong piezoelectric effect. © 2015 AIP Publishing LLC. [<http://dx.doi.org/10.1063/1.4929719>]

The rare earth ferroborates with the general formula $\text{RFe}_3(\text{BO}_3)_4$ ($\text{R}=\text{Y}$; La-Nd; Sm-Er) belong to a group of ferroelectric-magnetic materials (multiferroics) with combined magnetic ordering and ferroelectric properties. The development of antiferromagnetic ordering ($T_N \cong 30 - 40 \text{ K}$) leads to the simultaneous appearance of electrical polarization, i.e., nonintrinsic ferroelectricity. These materials are of interest because of their possible practical applications.¹ The ferroborates have served as convenient model systems for various physical studies over the last decade. An impressive amount of information has been gathered on their structure, magnetic, dielectric, magnetoelectric, magnetoelastic, and optical parameters.^{2,3}

There are, however, a number of “blank spots” in the published information on the ferroborates. (1) There are no systematic data on the magnitudes of the elastic moduli. The published data^{4,5} apply to particular cases and do not provide a general picture. (2) All compounds in this group belong to the non-centrally symmetric piezoelectric class D_3 , but almost nothing is known about the magnitudes of the piezoelectric moduli of the ferroborates, their temperature behavior, or their interactions with the magnetic subsystem. There is only one experimental paper⁶ in which the piezoelectric modulus of $\text{GdFe}_3(\text{BO}_3)_4$ is estimated based on measurements of the polarization charge during static loading at room temperature. These measurements showed that the piezoelectric modulus is a factor of two smaller than for α -quartz, and for that reason this compound was classified as a weak piezoelectric compound. Without making any specific comments on this conclusion, we note the possible hidden obstacles to the use of this⁶ method. Like all compounds of this crystalline class, the ferroborates tend to form enantiomorphic phases,⁷ which differ in the sign of some tensor components (including the piezoelectric modulus e_{11}), and if the measured response to it is linear, then it can be quenched in unfavorable circumstances.

Knowledge of the elastic and piezoelectric moduli is also important as a technical characteristic of these

compounds and for testing the theoretical schemes for calculating these properties. Here we note an attempt to calculate the lattice dynamics of holmium ferro- and alumoborates using the density functional method.⁸ It is clear from that article⁸ that there were insufficient experimental data to test the calculations, but, as will be shown below, we believe that this attempt was highly successful.

We have attempted to make systematic measurements of the elastic characteristics of some representatives of the family of ferroborates to determine the complete set of components of the elastic modulus tensor. The choice of the neodymium and samarium compounds was dictated by the relative simplicity of their behavior in the paramagnetic state, i.e., the absence of structural transitions, and the easy-plane character of the antiferromagnetic ordering.³ An additional stimulus⁹ for the study of samarium ferroborate was the discovery⁹ of giant magnetostriction (magnetostimulated features of its dielectric constant) in it. It may be assumed that similar effects occur in its piezoelectric response.

Here we present the results of acoustic measurements of the speeds of sound in these compounds in the para-phase. It turned out that the piezoelectric interaction is quite strong in them, so that not only the elastic moduli but the piezoelectric moduli could be extracted from the data on the sound speeds.

Single crystals, from which x-ray oriented samples were cut, were grown at the Institute of Physics of the Russian Academy of Science (Krasnoyarsk) by the method described in Ref. 10. The characteristic size of the samples was $\sim 2 \text{ mm}$.

The sound speeds were measured at liquid nitrogen temperature in a pulsed mode by a phase method, which is described in detail in Ref. 11. The working frequencies of the measurements were $\sim 55 \text{ MHz}$. The potential accuracy of the measurements in uniform samples for millimeter acoustic path lengths is better than 0.3%.

The piezoelectric interaction renormalizes the components of the Kristoffel tensor that defines the magnitude of the sound speed. In general, its elements are given by¹²

$$\Lambda_{ik} = C_{ilkm}n_l n_m + 4\pi \frac{(e_{l,mi}n_l n_m)(e_{p,qk}n_p n_q)}{\epsilon_{rs}n_r n_s}, \quad (1)$$

where C_{ilkm} is the elastic modulus matrix, n_i are the direction cosines of the wave normal vector, ϵ_{rs} is the dielectric tensor, and $e_{l,mi}$ is the piezoelectric modulus tensor which relates the polarization to the deformation which produces it ($P_i = e_{i,k}u_{kl}$). Equation (1) means that when the phase velocities of the acoustic oscillations are measured with sufficient accuracy for several directions of the wave normal, it is possible to recover all the elements of the tensors for the elastic moduli, as well as for the piezoelectric moduli. This type of program has, for example, been undertaken for lithium niobate.¹³

In class D_3 , to which all the ferroborates belong, five elements of the piezoelectric tensor are nonzero. Of these only two are linearly independent.¹² In Voigt's notation, these are

$$e_{11} = -e_{12} = -e_{26}, \quad e_{14} = -e_{25}. \quad (2)$$

$$\begin{pmatrix} \rho s^2 - (c_{66}n_2^2 + C_{44}n_3^2 + 2n_2n_3C_{14}) - \frac{4\pi(e_{11}n_2^2 + e_{14}n_2n_3)^2}{\epsilon_{11}n_2^2 + \epsilon_{33}n_3^2} & 0 & 0 \\ 0 & \rho s^2 - (C_{11}n_2^2 + C_{44}n_3^2 - 2n_2n_3C_{14}) & C_{14}n_2^2 - (C_{13} + C_{44})n_2n_3 \\ 0 & C_{14}n_2^2 - (C_{13} + C_{44})n_2n_3 & \rho s^2 - (C_{44}n_2^2 + C_{33}n_3^2) \end{pmatrix} \times \begin{pmatrix} u_x \\ u_y \\ u_z \end{pmatrix} = 0. \quad (4)$$

Except for the degenerate case ($n_3 = 1$), only the purely transverse mode with polarization parallel to the C_2 axis is piezoactive. For $q||z$, none of the modes are piezoactive.

The polarization in the sample can also be determined through a stress σ_{kl} applied to the sample: $P_i = d_{i,kl}\sigma_{kl}$. The components of the tensor $d_{i,kl}$ obey the same Eq. (2). It is easy to show that for hydrostatic compression ($\sigma_{kl} = p\delta_{kl}$), polarization does not develop in a sample. Physically, this is because hydrostatic compression does not change the lattice symmetry. As a result, the piezoelectric interaction does not affect the bulk compressibility and, independently of the boundary conditions (the crystal is shorted or open), the partial compressibilities are given by

$$K_x = K_y = \frac{C_{33} - C_{13}}{(C_{11} + C_{12})C_{33} - 2C_{13}^2},$$

$$K_z = \frac{C_{11} + C_{12} - 2C_{13}}{(C_{11} + C_{12})C_{33} - 2C_{13}^2}.$$

The isotropic compression modulus is given by

$$B = \frac{(C_{11} + C_{12})C_{33} - 2C_{13}^2}{C_{11} + C_{12} + 2C_{33} - 4C_{13}}. \quad (5)$$

The measurement algorithm consists of the following:

In order to carry out the program of finding all the components of the tensors Λ and e , we shall be interested in the sound speeds for wave normal directed along the x axis (the axis of symmetry C_2) and in the yz plane ($z||C_3$). In the first case ($n_1 = 1$) the Kristoffel matrix equation has the form

$$\begin{pmatrix} \rho s^2 - C_{11} - \frac{4\pi e_{11}^2}{\epsilon_{11}} & 0 & 0 \\ 0 & \rho s^2 - C_{66} & -C_{14} \\ 0 & -C_{14} & \rho s^2 - C_{44} \end{pmatrix} \begin{pmatrix} u_x \\ u_y \\ u_z \end{pmatrix} = 0, \quad (3)$$

i.e., in this geometry only the longitudinal mode is piezoactive.

For the wave normal lying in the yz plane ($n_1 = 0$), we have

-
- (1) From the longitudinal and transverse acoustic velocities s for $q||z$ ($n_3 = 1$), we determine C_{33} and C_{44} (Eq. (4));
 - (2) With the known C_{44} , the velocities of the quasilongitudinal and quasitransverse modes for $q||y$ ($n_2 = 1$) can be used to find C_{11} and $|C_{14}|$ (Eq. (4));
 - (3) From the velocity of the longitudinal mode for $q||x$ (for known C_{11} and ϵ_{xx}) we find e_{11} (Eq. (3));
 - (4) We find the value of C_{66} or C_{12} ($C_{12} = C_{11} - 2C_{66}$) using the velocity of the transverse mode for $q||y$ (with known e_{11});
 - (5) We calculated the remaining constants, C_{13} and e_{14} , from the measurements in turned y -cuts ($n_3 = n_2 = 1/\sqrt{2}$ or $n_3 = -n_2 = 1/\sqrt{2}$; Eq. (4)).

As noted above, the potential accuracy of the method used here in millimeter sized samples is better than 0.3%. However, despite our expectations, the program was hard to carry out in this case because of the strong inhomogeneity of the samples, especially of the samarium compound. Mode conversion on inhomogeneities leads to the appearance of secondary waves that interfere with the useful signal, so that the phase shift characteristic of the latter depends on the time of its arrival at the receiver interface. The major difficulty with the method used here¹¹ is determining the total number of wave lengths n superimposed on the sample length. We now discuss this point in more detail.

In this approach,¹¹ because a differential method is used, in its pure form it determines a fragment of the frequency dependence of the phase shift ($\delta\varphi = -\delta qL$, q is the wave number, and L is the acoustic path length) introduced by the sample. This dependence is approximated by a straight line (see Fig. 1), the slope of which is determined by the sound speed, but its actual position on the ordinate is only known to within $2\pi n$ (n is an integer). The velocity can be calculated from the slope of the line, but, because the frequency interval δf is small and set by technical limits, the accuracy of this estimate is sometimes not high enough. It can be increased by additionally requiring that the approximation line should intersect the ordinate at $2\pi n$. The optimum value of n is then determined by the condition that $2\pi n$ be as close as possible to the coordinate of the intersection of the initial (without the additional condition) approximation with the ordinate. This choice was tested by a statistical analysis. These arguments are, of course, only applicable to single-phase signals, for which the phase shift is linear with respect to frequency. Otherwise, the resultant phase depends on the ratio of the amplitudes of the signals participating in the process and its frequency dependence is more complicated; this is observed in nonuniform samples.

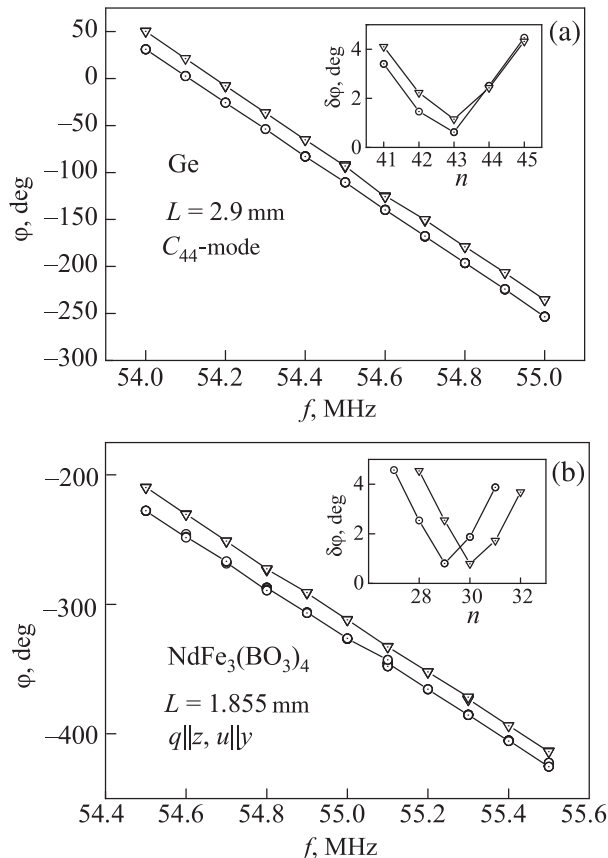


FIG. 1. Illustrating the method used to measure the sound speeds. (a) Phase-frequency characteristics of a fairly perfect single crystal of Ge taken from the positions of a strobe-pulse counter shifted by 10^{-7} s. The characteristics are shifted relative to one another by 20° . The inset shows the dependence of the standard deviations from the assumed number of integer wave lengths superimposed in the sample and determines the ordinate of the intersection of the approximation line (with the y axis). (b) The same for a single crystal of $\text{NdFe}_3(\text{BO}_3)_4$. The shift in the characteristics and the discrepancy in the minima of the standard deviations are caused by the variability of the phase shift introduced by the sample over the length of the measurement pulse.

We now illustrate these remarks with some examples. Figure 1(a) shows phase-frequency characteristics of a fairly perfect single crystal of Ge. These data were obtained for two readout positions of a strobe pulse separated by 10^{-7} s. In the figure the curves are separated vertically by 20° for ease of perception. The deviation of the intersection points of the approximation curve with the ordinate from a multiple of 2π does not exceed hundreds of degrees, so there is no doubt about the validity of the choice of $n = 43$. The optimal nature of this choice is confirmed by the inset in this figure: the mean square deviation is minimal for the chosen value of n , regardless of the position of the strobe-pulse counter. Because of the actual spread in the frequency interval, the accuracy of the velocity determination is better by more than an order of magnitude.

The typical situation for Nd ferroborate (not the worst version) is shown in Fig. 1(b). These data were obtained for the same shift in the strobe-pulse readouts. In this case, the mutual shift of the phase-frequency characteristics had already shown up in the measurements, and the discrepancy in the slopes is evident even to the naked eye. The inset in this figure indicates that the position of the minima of the mean square deviation depends on the position of the strobe pulse, so the value of n cannot be chosen with good justification.

These experiments showed that the degree of inhomogeneity depends on many factors that are not adequately monitored, such as the degree of squeezing of the crystal, the cooling rate, number of thermal cycles, etc. The phase distortions were especially strong in measurements of rotated y-cuts; this may be related to enantiomorphism of these compounds. Because of this, it was necessary to collect statistics and compare the results for samples with different lengths. In the latter case, there were two different sets of possible velocities which were assumed to be close to the true values. The limitations imposed by Eq. (4) were also taken into account: (a) the velocity of the QT-mode for $q||y$ must be lower than the velocity of the T-mode for $q||z$; (b) the squares of the velocities of the T-mode in y-cuts rotated by $\pm\pi/4$ must be greater than

$$\frac{1}{\rho} \left(\frac{C_{44} + C_{66}}{2} + \text{sign}(n_2)C_{14} \right).$$

We emphasize, however, that inhomogeneity had essentially no effect on the accuracy of measuring the velocities of longitudinal oscillations during data acquisition near the leading front of the first transmitted pulse, since all secondary waves are then slowed down relative to the primary signal. Since the signal at the pulse front depends fundamentally on the readout site, the measurement procedure has the distinctive feature described in Ref. 11.

The results of the velocity measurements are listed in Table 1.

To within the attainable accuracy, the sound speeds in the neodymium and samarium compounds were the same, so that measurements were not made in rotated y-cuts of the samarium ferroborate, where the effect of inhomogeneities was maximal.

The elastic and piezoelectric moduli are compared with calculated values for $\text{HoFe}_3(\text{BO}_3)_4$ (Ref. 8) in Table 2.

Here we clarify some points about Table 2.

TABLE 1. Velocities of sound (10^5 cm/s) in neodymium and samarium ferroborates.

n_1, n_2, n_3 Mode	0,0,1		1,0,0	0,1,0			0, 1/ $\sqrt{2}$, 1/ $\sqrt{2}$			0, -1/ $\sqrt{2}$, 1/ $\sqrt{2}$		
	L	T	L	QL	QT	T	QL	QT	T	QL	QT	T
NdFe ₃ (BO ₃) ₄	6.9	3.3	8.62	8.46	3.19	4.42	6.8	3.95	4.6	8.08	3.64	2.68
SmFe ₃ (BO ₃) ₄	6.9	3.35	8.7	8.52	3.25	4.27						

Note: L, T, QL, and QT denote the longitudinal, transverse, quasilongitudinal, and quasitransverse modes. The measurement accuracy for the longitudinal velocities is $\pm 0.5\%$. For the transverse velocities the most probable values are listed; these are estimated with an accuracy of $\pm 1.5\%$ but, because of possible errors in determining the total number of wavelengths superimposed on the sample length, deviations of 5%–7% are possible.

1. The numerical values of the moduli in Table 2 were obtained for a density of $\rho = 4.5$ g/cm³.
2. The sign of C_{14} depends on the choice of coordinate system. The theory of the elastic properties of crystals for class D_3 assumes a coordinate axis x directed along the C_2 axis,¹⁴ but the choice of its positive direction is not set by any symmetry considerations and requires additional supporting arguments. It is easy to see that for the two possible directions of the x axis the modulus C_{14} , like the piezoelectric modulus e_{11} , has a different sign. In α -quartz, which is symmorphic to the ferroborates, a positive emergence of the x axis is associated with the facet at which a positive polarization charge develops during strain deformation. The positive direction is also characterized by a certain sign of the rotation of the plane of polarization of light.¹⁵ Randomly or otherwise, for the additional assumption made here and the choice of x axis, the sign of C_{14} (in α -quartz) turns out to be positive. We have also taken the positive direction of the x axis to be that for which C_{14} is positive. This direction can be distinguished experimentally, and from the acoustic measurements, as Eq. (4) implies, in this case the sum of the squares of the velocities of the quasilongitudinal and quasitransverse modes in the rotated y -cut for $n_2 > 0$ is less than for $n_2 < 0$. In fact, this rule reduces to the following: for a correct choice of the direction of the x axis the velocity of the quasilongitudinal mode in these media is less when $n_2 > 0$. These experiments cannot be used to determine the sign of e_{11} ; it can only be said that for this choice of the direction of the x axis, the signs of e_{11} and e_{14} are the same in these compounds.
3. Calculating the piezoelectric moduli requires knowledge of the components of the dielectric tensor. For the samarium ferroborate, it was assumed that $e_{11} = 13.5$ (Ref. 9) and for the neodymium ferroborate, we used the values obtained from our own measurements ($e_{11} = 15$, $e_{33} = 22.5$).
4. The values of e_{11} for these compounds are essentially an order of magnitude greater than their analogs for quartz (4.3×10^5 CGSE vs. 5×10^4 CGSE for SiO₂ (Ref. 16)). We believe that this number is sufficiently reliable, since it is mainly derived from the reliably measured difference in the velocities of the longitudinal modes in the x - and y -

5. The modulus C_{13} can, in principle, be determined (for already known C_{11} , C_{33} , C_{44} , and C_{14}) using any value of the velocity for 45-degree rotated y -cuts taken from columns 8, 9, 11, and 12 of Table 1. The average of all the values obtained in this way is given in parentheses in column 6 of Table 2, where the confidence interval is represented by the spread in these values. It clearly goes beyond the possible errors and may be related to various factors: (a) to “unsuccessful” combination of enantiomorphic forms leading to mutual compensation of the contributions from regions with opposite signs for C_{14} ; (b) as in Ref. 17, to inaccurate orientation of the normal to the working facets of the sample in the yz plane. In the “ideal” case, for each cut the sum of the squares of the QL- and QT-modes times the density must be equal to

$$\frac{C_{11} + C_{13}}{2} + C_{44} - \text{sign}(n_2)C_{14}.$$

The first factor should lead to a reduction in the effective C_{14} , so that these sums should lie within a designated interval ($2C_{14}$). It can be seen from Tables 1 and 2 that this rule is not satisfied for $n_2 = -1/\sqrt{2}$. The correction associated with imprecise orientation can have an arbitrary sign for the deviation from the ideal case. For a small deviation ψ from the ideal direction, its value can easily be found using Eq. (4):

$$\rho \left(s_{QL}^2 + s_{QT}^2 \right) = \frac{C_{11} + C_{33}}{2} + C_{44} - \text{sign}(n_2)C_{14} + \psi \text{sign}(n_2)(C_{33} - C_{11}).$$

Of course, introducing the ψ -correction in the calculation of C_{13} yields one (the only) value when both modes are used for each cut. However, it turns out that the values of C_{13} found in this way for both cuts are essentially the same (column 6 of Table 2), so the values given there can be regarded as close to true. The deviations of the angles from 45° for these cuts were at a level of 4°–5°, entirely consistent with the possible errors in the method for preparing them in millimeter-sized samples. The resulting

TABLE 2. Elastic moduli (GPa) and piezoelectric moduli (C/m²) of the ferroborates.

Compound	C_{11}	C_{33}	C_{44}	C_{12}	C_{13}	C_{14}	B	e_{11}	e_{14}
NdFe ₃ (BO ₃) ₄	319	214	49	174	117 ± 3 (129 ± 21)	29.6	172	1.4 ± 0.3	0.4 ± 0.2
SmFe ₃ (BO ₃) ₄	324	214	50.5	194		28.6	175	1.4 ± 0.3	
HoFe ₃ (BO ₃) ₄ (Ref. 8)	370	159	68	125	72	30	130	0.99	0.11

corrections for inaccurate orientation were also used in the estimates of e_{14} .

6. A theoretical calculation for holmium ferroborate⁸ provides a qualitatively correct description of the basic features of the elastic characteristics of this class of compounds: enhanced rigidity in the base plane with respect to stress-strain deformations and a rather strong piezoelectric interaction.

We conclude with a summary of the basic results of this paper. The velocities of sound in single crystals of neodymium and samarium ferrobates in the paramagnetic state have been measured for a representative set of directions, which is sufficient to recover the elements of the tensors of the elastic and piezoelectric moduli. The elastic system is characterized by enhanced rigidity in the base plane with respect to stress-strain deformations. The intensity of the piezoelectric interactions is rather high and the piezoelectric moduli are an order of magnitude greater than the corresponding values for α -quartz.

^{a)}Email: fil@ilt.kharkov.ua

¹A. P. Pyatakov and A. K. Zvezdin, *Usp. Fiz. Nauk* **182**, 593 (2012).

²A. N. Vasil'ev and E. A. Popova, *Fiz. Nizk. Temp.* **32**, 968 (2006) [*Low Temp. Phys.* **32**, 735 (2006)].

³A. M. Kadomtseva, Yu. F. Popov, G. P. Vorob'ev, A. P. Pyatakov, S. S. Krotov, K. I. Kamilov, V. Yu. Ivanov, A. A. Mukhin, A. K. Zvezdin, A. M. Kuz'menko, L. N. Bezmaternykh, I. A. Gudim, and V. L. Temerov, *Fiz. Nizk. Temp.* **36**, 640 (2010) [*Low Temp. Phys.* **36**, 511 (2010)].

⁴G. A. Zvyagina, K. R. Zhekov, L. N. Bezmaternykh, I. A. Gudim, I. V. Bilych, and A. A. Zvyagin, *Fiz. Nizk. Temp.* **34**, 1142 (2008) [*Low Temp. Phys.* **34**, 901 (2008)].

⁵G. A. Zvyagina, K. R. Zhekov, L. N. Bezmaternykh, I. A. Gudim, I. V. Bilych, and A. A. Zvyagin, *Fiz. Nizk. Temp.* **36**, 376 (2010) [*Low Temp. Phys.* **36**, 296 (2010)].

⁶B. P. Sorokin, D. A. Glushkov, A. V. Kodyakov, L. N. Bezmaternykh, V. L. Temerov, and I. A. Gudim, *Vestnik KrasGU* **5**, 49 (2004).

⁷I. A. Gudim, V. L. Temerov, E. V. Eremin, N. V. Volkov, and M. S. Molokeev, "Racemism and macroscopic magnetoelectric effects in trigonal rare-earth oxyborates," in Abstracts of Talks at the V-th Baikal International Conf. on Magnetic Materials. New Technologies (Irkutsk, 2012), p. 82.

⁸V. I. Zinenko, M. S. Pavlovskii, A. S. Krylov, I. A. Gudim, and E. V. Eremin, *Zh. Eksp. Teor. Fiz.* **144**, 1174 (2013).

⁹A. A. Mukhin, G. P. Vorob'ev, V. Yu. Ivanov, A. M. Kadomtseva, A. S. Narizhnaya, A. M. Kuz'menko, Yu. F. Popov, L. N. Bezmaternykh, and I. A. Gudim, *Pis'ma v Zh. Eksp. Teor. Fiz.* **93**, 305 (2011).

¹⁰I. A. Gudim, E. V. Eremin, and V. L. Temerov, *J. Cryst. Growth* **312**, 2427 (2010).

¹¹E. A. Masalitina, V. D. Fil', K. R. Zhekov, A. N. Zholobenko, T. V. Ignatova, and S. I. Lee, *Fiz. Nizk. Temp.* **29**, 93 (2003) [*Low Temp. Phys.* **29**, 72 (2003)].

¹²L. D. Landau and E. M. Lifshitz, *Electrodynamics of Continuous Media* (Nauka, Moscow, 1982) [in Russian].

¹³A. P. Korolyuk, L. Ya. Matsakov, and V. V. Vasil'chenko, *Kristallografiya* **15**, 1028 (1970).

¹⁴F. I. Fedorov, *Theory of Elastic Waves in Crystals* (Nauka, Moscow, 1965) [in Russian].

¹⁵W. Cady, *Piezoelectricity and its Practical Applications* (IL, Moscow (1949) [in Russian].

¹⁶*Acoustic Crystals*, edited by M. P. Shaskol'skaya (Nauka, Moscow, 1982) [in Russian].

¹⁷T. N. Gaidamak, G. A. Zvyagina, K. R. Zhekov, I. V. Bilych, V. A. Desnenko, N. F. Kharchenko, and V. D. Fil', *Fiz. Nizk. Temp.* **40**, 676 (2014) [*Low Temp. Phys.* **40**, 524 (2014)].

Translated by D. H. McNeill